Journal of Power Sources 205 (2012) 318–323

Contents lists available at SciVerse ScienceDirect

Journal of Power Sources

journal homepage: www.elsevier.com/locate/jpowsour

Composition optimization of arc ion plated CrN_x films on 316L stainless steel as bipolar plates for polymer electrolyte membrane fuel cells

Min Zhang [a,c,*], Guoqiang Lin [b], Bo Wu [c], Zhigang Shao [c,**]

[a] School of Physics & Electronic Technology, Liaoning Normal University, Dalian 116029, China
[b] Lab of Material Modification by Laser, Ion, and Electron Beams, Dalian University of Technology, Dalian 116085, China
[c] Fuel Cell R&D Center, Dalian Institute of Chemical Physics, Chinese Academy of Sciences, Dalian 116023, China

ARTICLE INFO

Article history:
Received 14 October 2011
Received in revised form 4 January 2012
Accepted 4 January 2012
Available online 13 January 2012

Keywords:
Chromium nitride
Stainless steel bipolar plates
Arc ion plating
Interfacial contact resistance
Corrosion resistance

ABSTRACT

Thin films of CrN_x with different nitrogen contents are deposited on 316L stainless steel (SS316L) as bipolar plates for polymer electrolyte membrane fuel cells (PEMFCs) by arc ion plating (AIP) through adjusting nitrogen gas flow rate. The optimal N_2 flow rate and resultant N content in CrN_x films are determined by evaluating the interfacial contact resistance (ICR) between carbon papers and the coated samples, and the corrosion resistance in the simulated PEMFC conditions. After coating CrN_x films, the performance of SS316L bipolar plates is obviously improved, and has a close relationship with N content in the CrN_x films. Compared with the bare SS316L, the CrN_x coated SS316L exhibits a reduced ICR by one order of magnitude and the corrosion resistance increases by two orders of magnitude. The results show that $CrN_{0.86}$ film coated SS316L bipolar plates present best performance, i.e. the ICR of $CrN_{0.86}$ film coated sample reduces to 8.8 $m\Omega\,cm^2$ under 1.0 MPa compaction pressure, and the corrosion current density almost reaches 10^{-7} A cm^{-2}. The analysis indicates that the enhanced performance of the coated SS316L bipolar plates is related to the high film density determined by AIP, and the variation of phase structure and film composition.

1. Introduction

Polymer electrolyte membrane fuel cell is a device that directly and efficiently converts chemical energy into electricity with water as the only by-product. Due to its high efficiency and near-zero emission, PEMFC is of great interest as a clean energy device beyond petroleum [1]. Bipolar plate (BPP) is one of the most important and expensive components in a PEMFC stack and accounts to more than 80% of the total weight of the stack [2]. This multi-functional component not only serves as the backbone of serially connected cells, but also performs several other key functions such as conducting currents between cells, facilitating water and thermal management through the stack, and providing conduits for reactant gases [3]. Therefore, the BPP material must have good mechanical strength, low contact resistance with the backing, low gas permeability, inexpensive massive production and a low cost, be chemically stable, highly electrical and thermal conductive, and allow uniform reactant gas distribution and product removal.

Stainless steel is considered to be a promising candidate for bipolar plates in PEMFCs because of cost effectiveness, higher mechanical strength, better durability to shock and vibration, no permeability, and superior manufacturability compared to graphite composites [4]. Wang et al. [5] studied the performance of four types of stainless steel BPPs, e.g. 349^{TM}, 904L, 317L and 316L, and proposed that the performance of stainless steel bipolar plates improved with the increase in Cr content in the steels. However, during the operation of PEMFC stacks, BPP is exposed to a highly corrosive environment including F^-, SO_4^{2-}, SO_3^{2-}, and HSO_4^-. Upon the harsh acidic and humid environment inside the PEMFCs, bare metallic bipolar plates undergo the passivation process and a passive oxide film forms on the surface, which will increase the interfacial contact resistance (ICR) between bipolar plate and the adjacent gas diffusion layer (GDL). Furthermore, corrosion leads to a release of metal ions that can contaminate the electrolyte membrane and poison the electrode catalysts [6]. Both conditions can cause considerable degradation of stack performance.

To overcome the formation of surface oxide and the dissolution of metal in PEMFC environments, forming a protective and conductive coating by surface modification is regarded as an effective method and has been studied extensively [7–10]. However, many literatures [11,12] reveal that single modification layer fails

* Corresponding author at: School of Physics & Electronic Technology, Liaoning Normal University, Dalian 116029, China. Tel.: +86 411 84379508; fax: +86 411 84379185.
** Corresponding author at: Fuel Cell R&D Center, Dalian Institute of Chemical Physics, Chinese Academy of Sciences, Dalian 116023, China. Tel.: +86 411 84379153; fax: +86 411 84379185.
E-mail addresses: m.zhang@live.com (M. Zhang), zhgshao@dicp.ac.cn (Z. Shao).

0378-7753/$ – see front matter © 2012 Elsevier B.V. All rights reserved.
doi:10.1016/j.jpowsour.2012.01.056

to effectively protect metallic BPPs from corrosion because the layer, especially by physical vapor deposition (PVD) process, contains some defects like pinholes, pores and droplets, which tend to provide corrosion channels. To avoid this problem, we [13] developed and deposited a Cr/CrN/Cr multilayer with a sandwich-like structure on the SS316L bipolar plates for PEMFCs. The multilayer design introduces the interfaces between layers to block or disconnect the corrosion channels, thereby provides effective protection. The results show that the samples coated with Cr/CrN/Cr exhibit improved corrosion resistance and conductivity compared to bare SS316L samples. But the outmost Cr layer tends to passivate and a few Cr ions will dissolve and poison catalysts, which is unfavorable for PEMFC efficiency and lifetime. Cr/CrN multilayer will be employed in our future work to avoid this problem. Prior to doing this, the optimum of Cr/N content ratio in CrN films should be determined. Although some primary results on optimization of N_2 flow rate were obtained in our previous study [14], the mechanism involved was not discussed from a material and physical point of view.

In this paper, a series of CrN_x films with different nitrogen contents were deposited on 316L stainless steel as bipolar plates for PEMFCs by AIP through adjusting the nitrogen flow rate in order to further investigate the influence of Cr/N ratio on the performance of SS316L bipolar plates, and obtain the optimal value. The physical mechanism involved was discussed as well.

2. Experimental

The CrN_x films were deposited on the samples using an arc ion plating system, in which two opposite Cr targets of 99.9% pure and 55 mm in diameter were mounted at the end of linear ducts that connect to the chamber. Stainless steel holders lying in the center of the chamber can rotate and turn simultaneously. The distance between the center of the holder and the targets was 600 mm. A pulsed bias was applied on the holders through the axis.

Two kinds of samples are used as substrates, one is pure iron sheet with size of 20 mm × 10 mm × 1 mm, and the other is 316L stainless steel sheet for bipolar plates with size of 80 mm × 80 mm × 0.1 mm. The former is used for the measurement of the film composition and phase structure, and the latter one is for the evaluation of the contact resistance and anti-corrosion property of the coated samples. The substrates were ultrasonically cleaned in acetone, ethyl ethanol and deionized water subsequently for 15 min. Then they were blown dry and hung on the holders. The chamber was evacuated to a base pressure below 5.0×10^{-3} Pa using a turbo molecular pump and a rotary pump. Prior to the deposition, the samples were sputtered by Ar ions for 10 min with a pulsed bias of −800 V in ambient Ar at 2.0 Pa.

When the deposition began, two Cr targets were burnt by the triggers, and both arc currents were kept at 80 A. The partial pressure of Ar was kept at 0.5 Pa. The bias voltage, frequency and duty cycle of the pulsed bias were −300 V, 20 kHz and 40%, respectively. A pure chromium thin layer (approximately 30–50 nm) was deposited on the substrates as an interlayer to enhance the adhesion force. Then, nitrogen gas was introduced into the chamber, and reacted with chromium plasma evaporated from the targets, consequently forming CrN_x films on the substrates.

Five groups of CrN_x films with different nitrogen contents were deposited by adjusting the nitrogen gas flow rate, 10 sccm, 15 sccm, 20 sccm, 25 sccm and 50 sccm. The thickness of CrN_x films was controlled at approximately 1 μm by adjusting the deposition time.

The phase structure of films was identified by X-ray diffraction (XRD), film composition was measured by electron probe microscope analysis (EPMA) and the surface morphology was observed by scanning electron microscopy (SEM, JSM-5600LV).

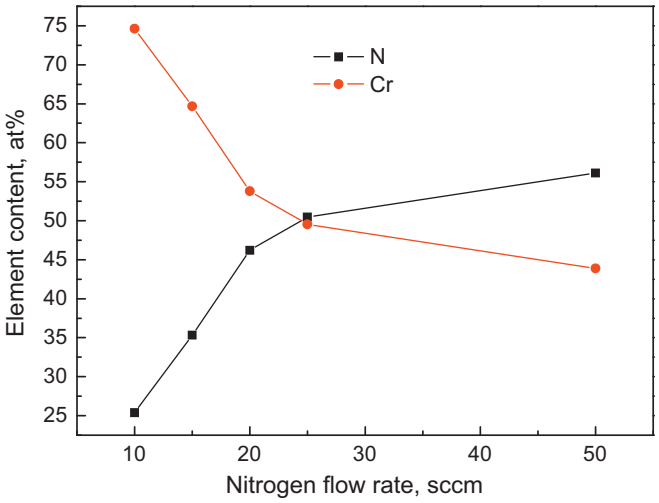

Fig. 1. The N and Cr element contents in the CrN_x films as a function of nitrogen gas flow rate.

The contact resistance between the CrN_x coated samples and gas diffusion layer (carbon paper) was measured with the conventional method extensively used by many researchers [5,15–17]. According to this method, two pieces of Toray carbon paper (TGP-H-060) were sandwiched between the samples and two gold-coated copper plates, on which an electrical current of 5.0 A, sourced by an INSTEK PSP-2010 programmable power supply was applied. During the tests, the compacting force was increased gradually at a step of 5 N s^{-1} controlled by a WDW electromechanical universal testing machine.

The corrosion resistance of the samples was evaluated at 25 °C by polarization electrochemical experiments using a potentiostat Model 2273A by EG&G Princeton Applied Research and analyzed with the corrosion software of EG&G Version 2.43.0. A 0.5 M H_2SO_4 with 2 ppm F^- solution was used as the corrosive solution to simulate an aggressive PEMFC operating environment. A conventional three-electrode system was used in the electrochemical measurements, in which a platinum sheet acted as the counter electrode, a saturated calomel electrode (SCE, sat'd KCl) as the reference electrode and the stainless steel sample as the working electrode. The size of the working electrodes was 15 mm × 15 mm × 0.1 mm. The edges were sealed by insulating epoxy resin, only leaving a 10 mm × 10 mm surface exposed to the electrolyte. The samples were stabilized at open circuit potential (OCP) for 10 min, and then the potential was swept from the OCP in the anodic direction at a scanning rate of 20 mV s^{-1}.

In order to evaluate the stability of the samples in the actual working conditions of PEMFCs, potentiostatic polarizations were performed in 0.5 M H_2SO_4 + 2 ppm F^- solution at 70 °C for over 6.5 h. Either air or H_2 was purged into the solution throughout the test to simulate the cathode or anode environment. During the measurements, the specimens were also stabilized at open circuit potential for 10 min. The current density as a function of time was recorded at applied anode (−0.1 V_{SCE}) and cathode (+0.6 V_{SCE}) potentials for PEMFCs.

3. Results

3.1. Film component

The N and Cr element contents in the CrN_x films as a function of nitrogen gas flow rate are shown in Fig. 1. Nitrogen content increases linearly when the nitrogen gas flow rate is in range of 10–20 sccm, but the increasing trend weakens above 20 sccm, till at 50 sccm, nitrogen content presents a saturation trend. Being the

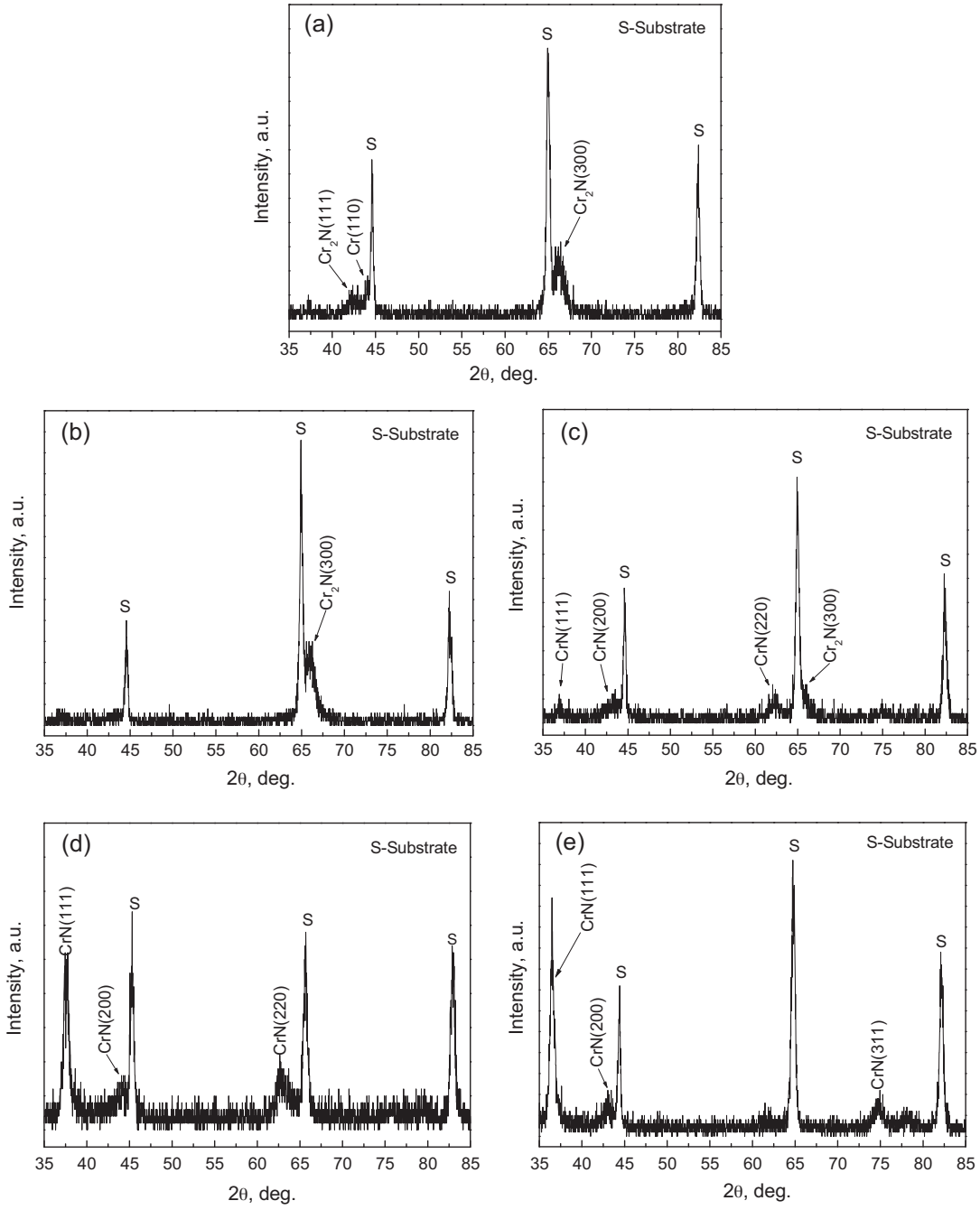

Fig. 2. XRD patterns of CrN_x films deposited with different N_2 flow rates of 10 sccm (a), 15 sccm (b), 20 sccm (c), 25 sccm (d) and 50 sccm (e).

other component of CrN, Cr content shows an opposite trend to N content as a function of nitrogen gas flow rate.

Table 1 summarizes N_2 flow rate, the resultant N and Cr contents in the CrN_x films, and the corresponding x values. It can be seen that the nitrogen content can be adjusted by changing the nitrogen gas flow rate, and N content in films rises from 25.4 at% to 56.1 at%, correspondingly, x value rises from 0.34 to 1.28, by increasing nitrogen gas flow rate from 10 sccm to 50 sccm.

Table 1
Summary of N_2 flow rate, the resultant N and Cr contents in the CrN_x films, and the corresponding x values.

Sample no.	N_2 flow rate (sccm)	N content (at%)	Cr content (at%)	x
S1	10	25.4	74.6	0.34
S2	15	35.3	64.7	0.55
S3	20	46.2	53.8	0.86
S4	25	50.5	49.5	1.02
S5	50	56.1	43.9	1.28

3.2. Phase structure

Fig. 2 shows XRD patterns of CrN_x films with different nitrogen contents. It indicates that phase structure of CrN_x films changes with the variation of nitrogen gas flow rate.

When nitrogen gas flow rate is 10 sccm, the film consists of Cr and Cr_2N phases. Although diffraction peaks of Cr phase are very weak, a small quantity of Cr phase indeed exists in the film. With the nitrogen gas flow rate increasing to 15 sccm, diffraction peaks from Cr phase disappear and the film mainly crystallizes into single Cr_2N

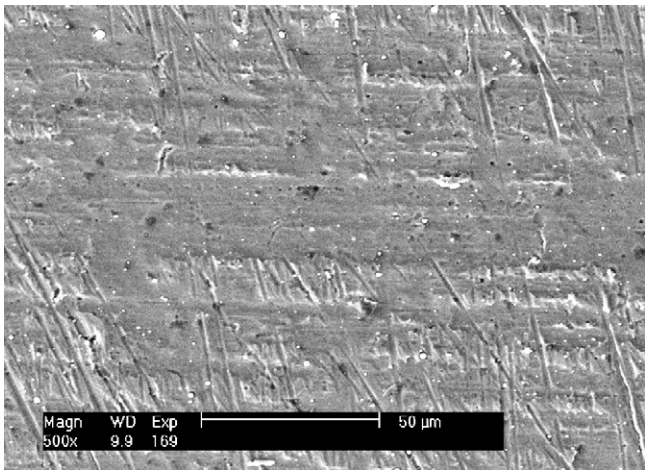

Fig. 3. Surface morphology of CrN_x film with 46.2 at% nitrogen content ($CrN_{0.86}$).

phase. As the nitrogen gas flow rate reaches 20 sccm, diffraction peaks from CrN phase obviously appear in the pattern, which indicates CrN phase forms in the film and the film consists of multiple Cr_2N and CrN phases. When the nitrogen gas flow rate is 25 sccm, only diffraction peaks of CrN are observed in the pattern, which shows the film is composed of single CrN phase. Finally, the nitrogen gas flow rate gets to 50 sccm, CrN (2 2 0) peak at 63° disappears, and CrN (3 1 1) peak appears at 75°, which means that increasing N_2 gas flow from 25 to 50 sccm does not result in a change of phase component, but of crystal orientation and film composition.

3.3. Surface morphology

The surface morphology of the CrN_x film with 46.2 at% nitrogen content ($CrN_{0.86}$) is shown in Fig. 3, and the other four samples exhibit the similar surface morphology with this. The substrate is industrial 316L stainless steel, and the films are very thin (only 1 μm in thickness), so there are many grooves and nicks on the coated sample surface, showing the typical characteristic of original stainless steel plates. Even so, it can be seen clearly from Fig. 3 that the films deposited by AIP are integrate and dense, adhered to the samples tightly, and no buckling and delamination are observed in the whole testing area.

3.4. Interfacial contact resistance

The contact resistance between bipolar plates and carbon papers as a function of compaction pressures is shown in Fig. 4. It is evident that the ICR between the sample and carbon paper decreases with increasing the pressure, and the variation trend weakens as the clamping pressure increases. The ICR between the CrN_x coated SS316L plates and carbon papers is obviously one order of magnitude lower than that between the bare SS316L plates and carbon papers (approximately 200 mΩ cm^2 at 8.0–1.0 MPa [11,13,18]). Transition metal nitrides such as CrN and TiN are metallic ceramics with good electrical conductivity [19,20]. XRD results obtained in this work show that chromium nitride coatings are formed on SS316L bipolar plates. The ICR of the coated plates is fairly low, indicating the conductivity of the bipolar plates is improved by coating chromium nitride films. This phenomenon is coincident with the results reported by many other researchers [21–23].

In this study, the $CrN_{0.86}$ coated sample shows better contact conductivity, the ICR being 8.8 mΩ cm^2 under a pressure of 1.0 MPa. The $CrN_{1.02}$ coated sample exhibits the highest ICRs, indicating poor contact conductivity.

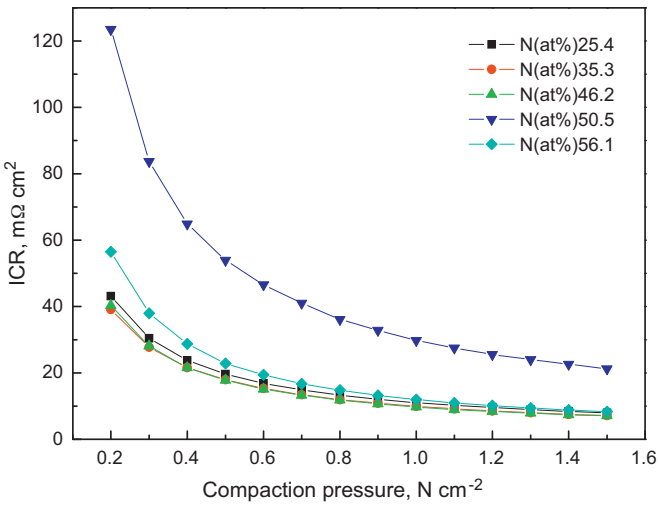

Fig. 4. ICRs of CrN_x coated SS316L bipolar plates under different compaction pressures.

3.5. Corrosion resistance

The potentiodynamic polarization curves of the CrN_x coated samples in the simulating corrosive solution are shown in Fig. 5. It is evident that the corrosion current density of the coated bipolar plates is lower than 10^{-5} A cm^{-2}, two orders of magnitude decreases compared with that of the original stainless steel (approximately 10^{-3} A cm^{-2}). The $CrN_{0.86}$ coated sample exhibits the lowest corrosion current density (around 10^{-7} A cm^{-2}), a higher breakdown potential (0.1 V), and the lowest passivation current density (lower than 10^{-6} A cm^{-2}). Thus, the $CrN_{0.86}$ coated sample shows the best corrosion resistance in simulating corrosive solution.

To further access the corrosion resistance of the CrN_x coated bipolar plates, a potentiostatic polarization study was performed for the optimized $CrN_{0.86}$ coated sample in simulating corrosive solution at 70 °C for over 6.5 h. The potentiostatic polarization curves for the $CrN_{0.86}$ coated 316L stainless steel in 0.5 M H_2SO_4 + 2 ppm F^- solution at anode and cathode potentials are respectively shown in Fig. 6(a) and (b). In both cases, the transient current density falls sharply upon the start of the polarization test, then gradually decreases, and lastly reaches a very low level as a steady state. The current density keeps stable at

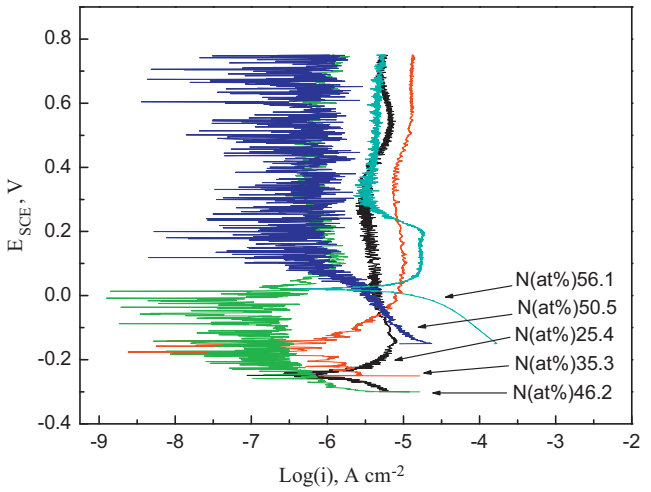

Fig. 5. Potentiodynamic polarization curves of the samples coated with CrN_x films with different N contents in 0.5 M H_2SO_4 with 2 ppm F^- at 25 °C.

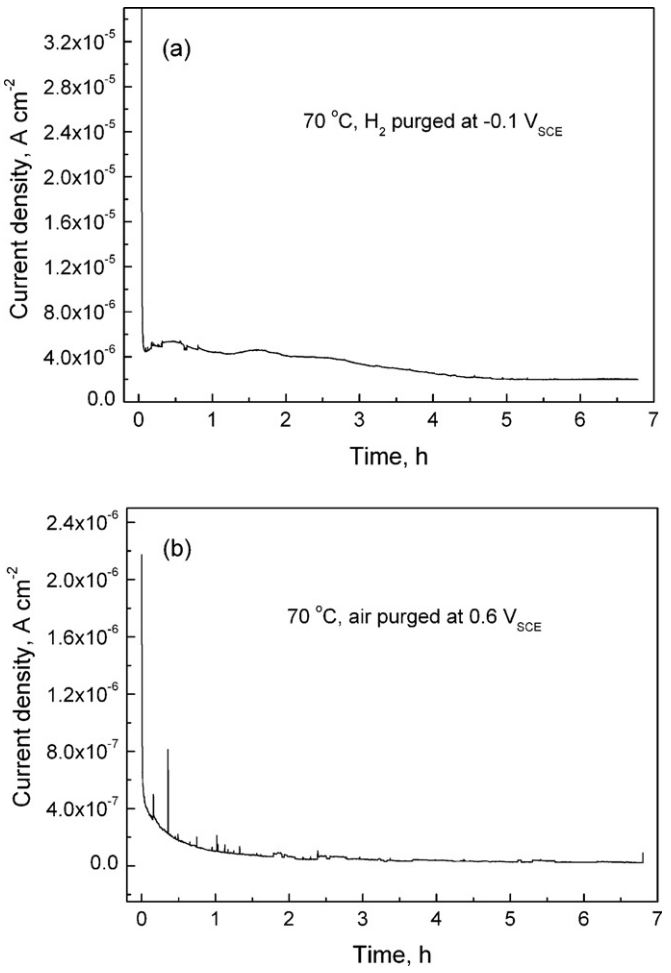

Fig. 6. Potentiostatic polarization curves of the samples coated with $CrN_{0.86}$ films in 0.5 M H_2SO_4 with 2 ppm F^- at 70 °C (a) purged with H_2 at −0.1 V_{SCE} and (b) purged with air at 0.6 V_{SCE}.

around 2.0×10^{-6} A cm^{-2} for the simulated anode environment, and 1.6×10^{-7} A cm^{-2} for the simulated cathode environment, which demonstrates that the CrN_x film with the optimized composition point ($x = 0.86$) deposited on 316L stainless steels is very stable in a PEMFC corrosion environment and provides adequate corrosion resistance for bipolar plates.

4. Discussion

All above results indicate that the contact conductivity and anti-corrosion property of five groups of stainless steel bipolar plates coated with CrN_x films are all obviously improved in comparison with those of the uncoated ones. It is attributed to the fact that CrN_x films deposited in this study replace the original passivation layer on the surface of stainless steel. The metallic compound CrN_x belongs to the conductive ceramic material, of which strength and corrosion resistance are similar to those of the passivation layer on stainless steel, namely Cr_2O_3, yet electrical conductivity of CrN_x films is much better. Therefore, bipolar plates coated with CrN_x films can not only maintain anti-corrosion property, but also decrease contact resistance. Furthermore, the fact that the films are good in quality, which means integrate and dense, adhered to the substrates tightly, guarantees the CrN_x films are playing their function well.

Additionally, the structure of films changes from multiple Cr/Cr_2N phases to single Cr_2N phase, and then to multiple CrN/Cr_2N phases, and finally to single CrN phase with increasing nitrogen gas flow rate, which is the main reason why the performance of the CrN_x coated samples changes with nitrogen gas flow rate. Generally speaking, if the corrosion resistance of a material is strong, take metal oxide for example, its electrical conductivity is worse. A material has good electrical conductivity, such as the pure metals, its corrosion resistance is poor. Corrosion resistance and electrical conductivity is a pair of contradiction for a material, and both are closely related to the state and behavior of free electrons in it [24–27]. It is necessary for free electrons in materials to be fewer or stable as possible to enhance the corrosion property. Oppositely, the free electrons are required to be more and active as possible to increase the electrical conductivity. For conductive metal nitrides with stoichiometric ratio, phase stability is highest, electric state density reaches the minimum near the Fermi level, and the density of electric free electrons is minimum, so the corrosion resistance is good and electrical conductivity is poor. As the composition deviates from the stoichiometric ratio or is doped with other element, its electrical conductivity will get better, but corrosion resistance will accordingly degrade. For CrN, it is possible to obtain three solid phases as the composition changes, which are chromium solid solution with a body-centered-cubic structure, Cr_2N with a hexagonal crystal structure, and CrN with a face-centered-cubic structure. And x value in these three phases is 0, 0.5 and 1.0, accordingly. The electrical conductivity declines and corrosion resistance enhances in order of Cr, $CrN_{0.5}$, $CrN_{1.0}$. It can be confirmed in Fig. 5 that the passivation current of the $CrN_{1.02}$ coated sample is less than 10^{-6} A cm^{-2}, as low as that of $CrN_{0.86}$, indicating a good corrosion resistance. When the film is deposited with the composition point deviated from the point of stoichiometric ratio, multiple phase mixture and deviation in composition will cause a variation in the density of free electrons, which inevitably leads to a change in electrical conductivity and corrosion resistance. The $CrN_{0.86}$ film obtained in this work exhibits the suitable composition point, with which chromium nitride with good electrical conductivity and corrosion resistance is obtained. In addition, the mixture of CrN and Cr_2N is contributed to the improved performance of the $CrN_{0.86}$ coated samples.

5. Conclusions

Thin films of CrN_x with different nitrogen contents are deposited on SS316L bipolar plates by AIP through adjusting the nitrogen gas flow rate, and nitrogen content in the obtained films changes from 25.4 at% to 56.1 at%, correspondingly, x value in CrN_x changes from 0.34 to 1.28. The performance of the CrN_x coated samples is obviously improved compared to the bare SS316L plates. The corrosion resistance increases by more than two orders of magnitude and the ICR decreases by one order at least. The composition and phase structure of the films change as a function of the nitrogen content, which directly influences the ICR and corrosion resistance of the coated plates. The $CrN_{0.86}$ film coated SS316L bipolar plates present the best performance, i.e. the ICR of $CrN_{0.86}$ film coated sample reduces to 8.8 mΩ cm^2 at 1.0 MPa compaction pressure, and the corrosion current almost reaches 10^{-7} A cm^{-2}.

Acknowledgements

This work was financially supported by the China Postdoctoral Science Foundation (Grant No. 20110491545), National Natural Science Foundation of China (Grant No. 51101080), and Program for Liaoning Excellent Talents in University (Grant No. LJQ2011115).

References

[1] B.C.H. Steele, A. Heinzel, Nature 414 (2001) 345–346.

[2] A. Kumar, J. Power Sources 129 (2004) 62–67.
[3] H. Tawfik, Y. Hung, D. Mahajan, J. Power Sources 163 (2007) 755–767.
[4] H. Wang, J.A. Turner, Fuel Cells 10 (2010) 510–519.
[5] H. Wang, M.A. Sweikart, J.A. Turner, J. Power Sources 115 (2003) 243–251.
[6] Y. Wang, D.O. Northwood, J. Power Sources 165 (2007) 293–298.
[7] C.-Y. Bai, T.-M. Wen, M.-S. Huang, K.-H. Hou, M.-D. Ger, S.-J. Lee, J. Power Sources 195 (2010) 5686–5691.
[8] J. Liu, F. Chen, Y. Chen, D. Zhang, J. Power Sources 187 (2009) 500–504.
[9] S.Y. Kim, D.H. Han, J.N. Kim, J.J. Lee, J. Power Sources 193 (2009) 570–574.
[10] C.-Y. Chung, S.-K. Chen, P.-J. Chiu, M.-H. Chang, T.-T. Hung, T.-H. Ko, J. Power Sources 176 (2008) 276–281.
[11] L. Wang, D.O. Northwood, X. Nie, J. Housden, E. Spain, A. Leyland, A. Matthews, J. Power Sources 195 (2010) 3814–3821.
[12] D. Zhang, L. Duan, L. Guo, W.-H. Tuan, Int. J. Hydrogen Energy 35 (2010) 3721–3726.
[13] M. Zhang, B. Wu, G. Lin, Z. Shao, M. Hou, B. Yi, J. Power Sources 196 (2011) 3249–3254.
[14] Y. Fu, G. Lin, M. Hou, B. Wu, H. Li, L. Hao, Z. Shao, B. Yi, Int. J. Hydrogen Energy 34 (2009) 453–458.
[15] D.P. Davies, P.L. Adcock, M. Turpin, J. Power Sources 86 (2000) 237–242.
[16] A. Pozio, F. Zaza, A. Masci, R. Silva, J. Power Sources 179 (2008) 631–639.
[17] S.B. Lee, K.H. Cho, W.G. Lee, H. Jang, J. Power Sources 187 (2009) 318–323.
[18] D.H. Han, W.H. Hong, H.S. Choi, J.J. Lee, Int. J. Hydrogen Energy 34 (2009) 2387–2395.
[19] S. Seal, JOM 9 (2001) 51–54.
[20] W.J. Meng, T.J. Curtis, J. Electron. Mater. 26 (1997) 1297–1302.
[21] M.P. Brady, H. Wang, B. Yang, J.A. Turner, M. Bordignon, R. Molins, M. Abd Elhamid, L. Lipp, L.R. Walker, Int. J. Hydrogen Energy 32 (2007) 3778–3788.
[22] Y. Fu, M. Hou, G. Lin, J. Hou, Z. Shao, B. Yi, J. Power Sources 176 (2008) 282–286.
[23] B.-C. Cha, Y.-Z. You, S.-T. Hong, J.-H. Kim, D.-W. Kim, B.-S. Lee, S.-K. Kim, Int. J. Hydrogen Energy 36 (2011) 4565–4572.
[24] B. Wu, PhD Dissertation in Plasma Physics, Dalian Univ of Technol, Dalian, 2010.
[25] C. Kittel, Introduction to Solid State Physics, 7th edition, John Wiley & Sons, Inc., New York, 1996.
[26] N.W. Ashcroft, N.D. Mermin, Solid State Physics, Harcourt College Publishers, 1976.
[27] M. Zhang, G. Lin, L. Hu, Z. Shao, J. Power Sources 198 (2012) 196–202.